Optics Letters

208 W single-frequency 1064 nm laser based on a single-crystal fiber master-oscillator power amplifier

Yixiao Wei,[1] Weina Peng,[1] Jiawei Li,[1] Pixian Jin,[1,2] Jing Su,[1,2] and Huadong Lu[1,2,*]

[1]State Key Laboratory of Quantum Optics and Quantum Optics Devices, Institute of Opto-Electronics, Shanxi University, Taiyuan 030006, China
[2]Collaborative Innovation Center of Extreme Optics, Shanxi University, Taiyuan 030006, China
*luhuadong@sxu.edu.cn

Received 18 January 2024; revised 1 March 2024; accepted 1 March 2024; posted 4 March 2024; published 18 March 2024

High-power all-solid-state continuous-wave (CW) single-frequency laser with high linear polarization is a significant source for quantum optics and precision measurement. In this Letter, a high-power linearly polarized CW single-frequency laser based on the single-crystal fiber (SCF) master-oscillator power amplifier (MOPA) is presented, in which a homemade 140 W low-noise CW single-frequency laser and a Nd:YAG SCF are firstly employed as the seed laser and the medium of the MOPA, respectively. The mode-matching between the pump laser propagated with waveguide form and the freely propagated seed laser is optimized by considering the influence of the degradations of the polarization and the beam quality. Finally, when the incident powers of the pump and seed lasers are 262.6 W and 126.3 W, respectively, the seed waist radius is optimized to 200 μm. In this case, the output power of the linearly polarized laser reaches up to 208 W, which is the highest output power, to the best of our knowledge. The presented results provide a good reference for implementing a high power and high degree of the polarization and good beam quality laser based on the SCF MOPA. © 2024 Optica Publishing Group

https://doi.org/10.1364/OL.519212

All-solid-state continuous-wave (CW) single-frequency lasers have widespread applications in cold atom physics, quantum secure communication, high-precision measurement, and so on due to their intrinsic advantages of good beam quality, high stability, and low-intensity noise. Especially, with the rapid development of science and technology, it is urgent to scale up the output power of an all-solid-state CW single-frequency laser. For example, a CW single-frequency laser with high output power can be used to pump multiple optical parametric oscillators at the same time for obtaining multi-partite entangled states which paves a way to develop quantum network and quantum computation [1]. In the application of laser interferometer gravitational-wave observatory (LIGO), the output power of the all-solid-state single-frequency CW laser injected into the LIGO device should reach up to 200 W to improve the detection sensitivity of the device by 10 times relative to the initial LIGO with 10 W injected laser [2].

So far, scaling up the output power of the single-frequency CW laser is mainly implemented by means of laser amplifiers including main oscillation power amplifier (MOPA) and seed injection locking amplifier, where the fiber, slab, thin disk, and rod/bulk crystal usually act as the laser media. A CW single-frequency laser with the maximum output power of 811 W has been achieved by Robin *et al.* in 2014, which was implemented by adopting a photonic crystal fiber amplifier [3]. However, due to the core diameter of the fiber which was usually as small as 5–40 μm, the intensity noises caused by the stimulated Brillouin scattering (SBS) and stimulated Raman scattering (SRS) in the fiber amplifier will become more and more serious with the increase of the output power of the laser system. The existence of these noises would directly hinder its possible applications in highly precise devices. For the slab amplifier, in order to achieve high gain and good thermal management, the incident end surface is made in the slender shape which is much smaller than both heat dissipating faces. In 2021, a 148.1 W single-frequency quasi-continuous-wave 1064 nm laser was reported by Zhang *et al.*, which was demonstrated by utilizing a partially pumped slab amplifier [4]. The pump beam had to be shaped into a homogenous line shape with a size of 15 × 0.6 mm^2 to cover the incident pump surface of the slab gain medium, and the seed laser also had to be shaped into an elliptical beam for realizing the good mode-matching with the shaped pump beam. As a result, the asymmetrical thermal lens effect in the slab gain medium occurs and inevitably induces the large divergence in a direction. The thin-disk laser amplifier generally employs a thin disk with a large pump end surface and small thickness of hundred-micrometer level as the gain medium, and the whole surface is adhered together with a water-cooled heat sink. The seed laser and the pump beam are reflected and transmitted multiple times in the thin-disk crystal to obtain high enough gain and good heat dissipation. The thin-disk amplifiers have been widely applied in the field of kW-class pulsed lasers [5]. However, lots of mirrors are employed to realize multi-pass amplification, and the position of every mirror and the angle of the incident laser beam must be precisely aligned, which causes the complicated structure and increases the difficulty of design and debugging. Compared to other types of amplifiers, the rod/bulk amplifiers possess apparent advantages of perfect beam quality, low noise, high power stability, and narrow linewidth. To overcome the thermal lens effect and avoid the damage of the rod/bulk laser crystal, two or more gain media have been employed for scaling up the output power of a laser amplifier. In 2020, a laser

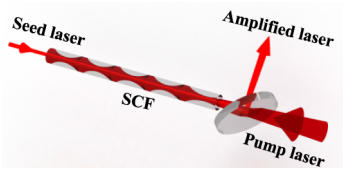


Fig. 1. Transmission diagram of the seed laser and the pump laser in the SCF.

amplifier system of 195 W based on two sequential MOPAs with four-stage single-pass Nd:YVO_4 crystals and the seed laser of 35 W was reported by Bode *et al.* [6].

Recently, as a combination of a rod crystal with a conventional fiber, the single-crystal fiber (SCF) with highly stimulated Brillouin scattering threshold, excellent thermal management, and pump waveguide effect has become a more and more popular candidate to scale up the output power. Especially, in 2012, Délen *et al.* demonstrated a 250 W CW laser under the pump power of 600 W based on a standing wave cavity [7]. Although the mode-matching efficiency has been calculated, the attained beam quality factor was as large as 15. In 2022, Chen *et al.* presented a single-frequency 1064 nm laser based on Nd:YAG SCF MOPAs, but the output power was limited to 60.4 W due to the low seed power of 0.7 W [8]. In order to scale up the output power of the CW single-frequency linearly polarized 1064 nm laser based on the Nd:YAG SCF, it is necessary to increase the powers of the seed laser and the pump laser. In this Letter, a homemade 140 W low-noise CW single-frequency laser and a Nd:YAG SCF are firstly employed as the seed laser and the medium of the MOPA, respectively. In the experiment, we find that due to the isotropy of the Nd:YAG SCF, severe thermal lens effect and thermal birefringence effect can still cause the depolarization and the beam quality degradation of the seed laser with the increase of the powers of the seed and pump lasers even though the thermal management ability of the SCF is better than that of the traditional Nd:YAG bulk crystal. As a result, the polarization degree and the beam quality factor of the obtained laser after SCF amplification will be severely degraded. In order to obtain a CW high-power single-frequency 1064 nm laser with high linear polarization degree and good beam quality based on a SCF MOPA, the degradations of the polarization and the beam quality should be taken into account. After the mode-matching is optimized by considering the influence of the degradation of the polarization and the beam quality on the optical conversion efficiency, a CW single-frequency linearly polarized 1064 nm laser with an output power of 208 W is achieved, which is the highest output power, to the best of our knowledge.

When the seed laser and the pump laser are simultaneously injected into the SCF from the front and rear surfaces, respectively, as shown in Fig. 1, the seed laser propagates in the SCF freely, while the pump laser propagates with the waveguide form due to the side reflection of the SCF. In this case, it is necessary to firstly optimize the mode-matching efficiency between the seed and pump lights for attaining a high optical conversion efficiency. It is well known that the mode-matching efficiency between the pump and seed lights can be calculated according to the normalized overlap integral [9]:

$$\eta = \frac{|\int E_p E_s dA|^2}{\int |E_p|^2 dA \int |E_s|^2 dA}, \tag{1}$$

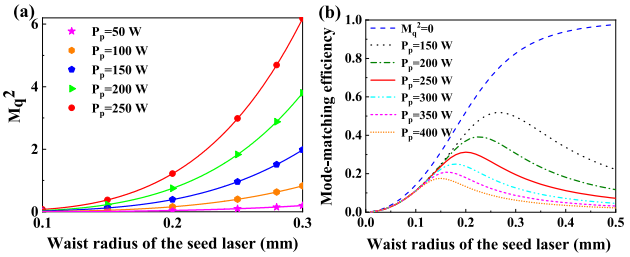


Fig. 2. (a) Dependence of the M_q^2 on the seed waist radius for the different incident pump powers. (b) Mode-matching efficiency between the pump and seed lasers depends on the seed waist radius for the different incident pump powers.

where E_p and E_s are the electric field distributions of the pump light and the seed light, respectively, and simply expressed as $E_{s,p}=[I_{s,p}(r)]^{1/2}$. For the seed laser, its initial normal Gaussian distribution will be disturbed with the increase of the incident pump power because of the thermal lens effect and the thermal birefringence effect, so the intensity distribution of the seed laser can be expressed as [10]

$$I_s(r) = \frac{2P_s}{\pi\omega_s^2} e^{\frac{-2r^2}{\omega_s^2}}, \tag{2}$$

where

$$\omega_s = \frac{\omega_{s0}}{\sqrt{M_s^2}} \tag{3}$$

and

$$M_s^2 = \sqrt{(M_i^2)^2 + (M_q^2)^2}. \tag{4}$$

ω_{s0} is the initial waist radius of the seed light. M_i^2 is the initial beam quality of the seed laser (1.23). M_q^2 is the additional contribution to the beam quality factor caused by the quartic-phase aberration effects, and it is induced by the parabolic pump distribution and the variation of thermal conductivity dependent on temperature [11–14]. The parabolic pump distribution can be converted and expressed based on the expression of the heat intensity given in [11]:

$$I_p(r) = \frac{P_p}{\pi\omega_p^2} \frac{1}{(1-\beta/2)} (1 - \frac{\beta}{b^2} r^2), \tag{5}$$

where

$$\omega_p = \omega_{p0} \sqrt{1 + (\frac{M_p^2 \lambda_p (z - z_0)}{n\pi\omega_{p0}^2})^2}. \tag{6}$$

β is the parameter for the pump inhomogeneity (0.15) [11]. b is the radius of the SCF. ω_{p0} is the waist radius of the pump light; λ_p and n are the wavelength of the pump light and the refractive index of the SCF (1.82), respectively; and the beam quality factor M_p^2 of the pump light is approximately 170. Figure 2(a) depicts the relationship between the M_q^2 and the waist radius of the seed laser for the different incident pump powers. It can be seen that the M_q^2 will increase quickly with the increase of the incident pump power. Moreover, for the same incident pump power, the larger the waist radius of the seed laser, the larger the value of the M_q^2. At the same time, substituting Eqs. (2)–(6) into Eq. (1), the mode-matching efficiency between the pump beam and the seed beam in the SCF is illustrated in Fig. 2(b). It is clear that without considering the degradation of the beam quality, the larger the beam waist spot of the seed light, the

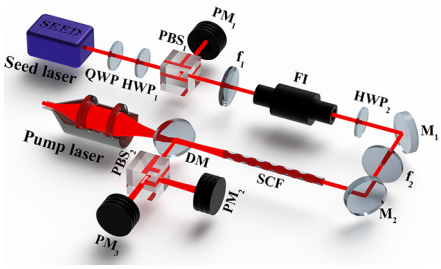


Fig. 3. Schematic diagram of the Nd:YAG SCF MOPA.

higher the mode-matching efficiency between the seed and pump lights, as shown by the blue dotted line in Fig. 2(b). However, there is an optimal waist size for the seed laser to obtain a maximum optical conversion efficiency once the degradation of beam quality is taken into account. Moreover, the higher the incident pump power, the smaller the optimal beam waist spot, and the smaller the difference value of the optimal beam waist spot of the seed laser corresponds to the same difference value pump power. Especially, from Fig. 2(b), it can be seen that the optimal waist radius of the seed laser is 200 μm for the incident pump power of 262.6 W.

According to the calculated results, a high-power linearly polarized CW single-frequency laser based on the Nd:YAG SCF MOPA is built, and the schematic diagram is shown in Fig. 3. The seed laser is a homemade low-noise all-solid-state CW single-frequency 1064 nm laser with the output power and linewidth of 140 W and 102 kHz, respectively [15]. The polarization degree of the output seed laser is firstly improved by employing a quarter-wave plate (QWP). Then, a power adjuster composed of a half-wave plate (HWP) and a polarization beam splitter (PBS) is utilized to control the incident power of the seed laser injected into the amplifier. The leaked seed light from the power adjuster is collimated and focused by two aspherical lenses f_1 ($f_1 = 300$ mm) and f_2 ($f_2 = 350$ mm) and then injected into the designed MOPA to achieve the optimal mode-matching. To prevent the reflected light of the amplifier from damaging the seed laser, a commercial Faraday isolator (IO-10-1064-VHP, Thorlabs) is placed between the seed laser and the SCF. The core of the built MOPA is a Nd:YAG SCF with the diameter of 1 mm and the length of 50 mm, respectively. The Nd^{3+} doping concentration is 0.2 at.%. Both end-faces are coated with anti-reflection (AR) films at both 1064 nm and 808 nm. To attain the good heat dissipation as soon as possible and effectively control the temperature of the SCF, the SCF is closely wrapped with an indium foil and enclosed by water-cooled copper blocks when it is end-pumped by a fiber-coupled laser diode (LIMO, LIMO400-f400-DL808-EX1815) with the center wavelength at 808 nm and the maximal output power of 400 W. The diameter and the numerical aperture (NA) of the coupling fiber are 400 μm and 0.22, respectively. The incident pump laser is also shaped by a telescope system to an approximate pump spot of 600 μm in diameter and then injected into the SCF. The beam waist of the pump laser is positioned a few millimeters at the rear surface of the SCF, and the pump beam is guided by the internal reflection inside the SCF. The seed light and the pump light are contra-propagative instead of co-propagative, which well reduces the influence of the thermal effect and the damage probability of the SCF. Flat folding mirrors M_1 and M_2 with 45° incident angle are coated with high-reflection (HR) film at 1064 nm. The dichroic mirror (DM) coated with HR at 1064 nm and

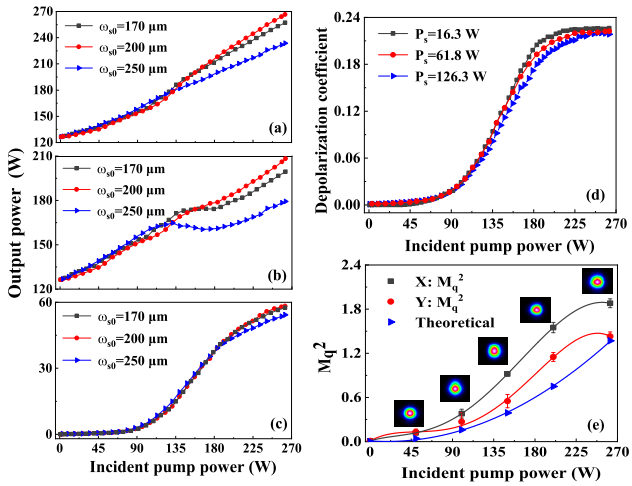


Fig. 4. (a) Total output power. (b) Output power of the linearly polarized laser. (c) Output power of the depolarization laser. (d) Dependences of the depolarization coefficient on the incident pump power for different seed powers. (e) Variations of the M_q^2 values and the spatial beam profiles with the increase of the incident pump power.

high transmission (HT) at 808 nm is used to separate the amplified laser from the pump light and acts as the output mirror of the amplifier. To realize linearly polarized laser output, a PBS is employed to filter out the depolarized beam. In the experiment, the waist radius of the seed laser beam in the SCF is changed from 170 μm to 200 μm and 250 μm by replacing the focusing lens. The total output power and the powers reflected as well as leaked from the PBS are recorded and shown in Figs. 4(a)–4(c), where the incident power of the seed laser is 126.3 W. It is clear that the output power is basically the same when the incident pump power is lower than 120 W. However, once the incident pump power is higher than 120 W, the influence of the waist size of the seed laser on the output power of the SCF MOPA becomes more and more severe with the increase of the incident pump power. When the waist radius of the seed laser is 200 μm, the total output power can reach up to 266.5 W, and the corresponding extraction efficiency is up to 53.3%. In this case, the power of the horizontal polarization laser leaked from the PBS is 208.2 W. In other words, there is a 58.3 W laser simultaneously generated due to the depolarization, which is reflected from the PBS. However, when the waist radius of the seed laser is adjusted to 170 μm or 250 μm, the total output powers are only 257.1 W and 233.6 W, respectively, which are lower than that of 266.5 W for the 200 μm beam waist. At the same time, the corresponding extraction efficiencies also reduce to 49.8% and 40.9%, respectively. Moreover, the output powers of the linearly polarized 1064 nm laser leaked from the PBS reduce to 199.5 W and 179.3 W, respectively. In addition, the depolarization as a function of the incident pump power with different incident seed powers is depicted in Fig. 4(d) when the beam radius of the seed laser is 200 μm. It is clear that the depolarization is almost negligible when the incident pump power is below 70 W. However, once the incident pump power is above 70 W, the depolarization rapidly increases to about 0.22 and tends to saturate with the increase of the incident pump power. Figure 4(d) shows that the power of the seed laser has little effect on the depolarization. In other words, the depolarization is mainly caused by the incident pump power. Furthermore, the variations of the M_q^2 values and

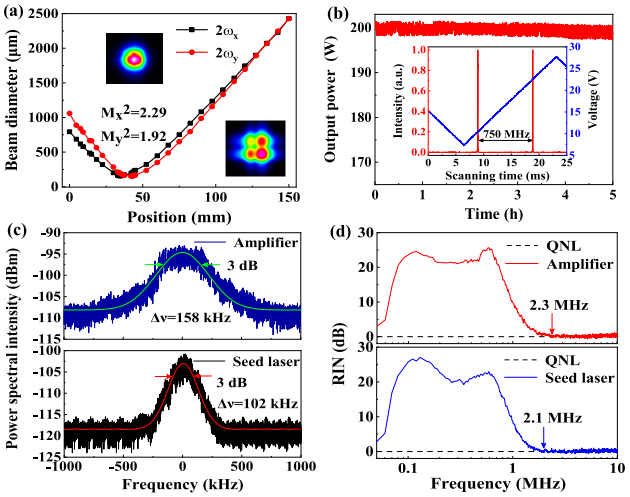


Fig. 5. (a) Transverse-mode characteristic. (b) Power stability for 5 h and longitudinal-mode structure. (c) Linewidth. (d) Relative intensity noise (RIN) spectrum.

the corresponding spatial beam profiles of the linearly polarized laser with the increase of the incident pump power are also measured when the waist radius of the seed laser is 200 μm, which is depicted in Fig. 4(e). It is also seen that the additional contribution of the beam quality factor M_q^2 can quickly increase with the increase of the incident pump power. Once the incident pump power is above 100 W, the M_q^2 is slightly larger than the theoretical calculation values, which is attributed to the polarization interferometer induced by depolarization and the thermal lens effect caused by the bulged entrance and exit faces. From Fig. 4, it is clear that the experimental results are in good agreement with the previous theoretical calculation, which reveals that it is necessary to optimize the mode-matching between the incident seed and pump lasers when a SCF is used as the MOPA medium. The optimal waist radius of the seed laser is 200 μm when the incident pump power and the seed power are 262.6 W and 126.3 W, respectively. In this case, the caustic curve and corresponding spatial beam profile of the 1064 nm laser are measured by a beam quality analyzer (M2SETVIS, Thorlabs). Figure 5(a) shows that the measured beam quality factors in the X and Y directions are 2.29 and 1.92, respectively, and the spatial beam profile of the depolarization laser is also measured and shown in the bottom right of Fig. 5(a). The peak-to-peak power fluctuation of the linearly polarized laser is recorded in Fig. 5(b), which is lower than ±1% in 5 h. Since a small part of the linearly polarized laser is used to implement other performance measurements including the transverse-mode characteristic, longitudinal-mode structure, linewidth, and relative intensity noise spectrum, the recorded power value depicted in Fig. 5(b) is lower than the actual output power of 208 W. At the same time, the longitudinal-mode structure is monitored by employing a homemade Fabry–Perot cavity with a free spectral range of 750 MHz in the amplification process, and the monitored result is depicted in the inset of Fig. 5(b), which shows that the amplifier always maintains stable single-longitudinal-mode operation. The linewidth and the relative intensity noise (RIN) of the linearly polarized laser are also measured and recorded in Figs. 5(c) and 5(d), respectively. It can be seen that the measured linewidth is as narrow as 158 kHz, and the linewidth broadening is only 56 kHz compared to the seed laser. The cutoff frequency that the laser reaches the quantum noise limit (QNL) is 2.3 MHz. The frequency and amplitude above the QNL for the resonant relaxation oscillation (RRO) peak are 590 kHz and 25.6 dB, respectively. The frequency that reached the QNL is only shifted back (0.2 MHz), and the amplitude of the RRO peak above the QNL is amplified (2.8 dB) as compared to the seed laser. From these experimental results, it is clear that there is no obvious nonlinear effect in the amplification process.

In conclusion, we present a high-power linearly polarized CW single-frequency 1064 nm laser based on the SCF MOPA, in which a homemade 140 W low-noise CW single-frequency laser and a Nd:YAG SCF act as the seed laser and the laser medium of the MOPA, respectively. In order to obtain a high conversion efficiency, it is necessary to optimize mode-matching efficiency between the incident pump and seed lasers by considering the influence of the degradations of the polarization and the beam quality. From the theoretical calculation, it is found that there is an optimal seed laser waist size for the different incident pump powers after the degradation of the beam quality is taken into account. The experimental results are in good agreement with the theoretical calculation. Finally, when the incident powers of the pump and seed lasers are 262.6 W and 126.3 W, respectively, the seed waist radius is optimized to 200 μm. In this case, the output power of the linearly polarized laser reaches up-to 208 W, which is the highest output power, to the best of our knowledge. The presented results provide a good reference for implementing a high power and high degree of the polarization and good beam quality laser based on the SCF MOPA technique.

Funding. National Natural Science Foundation of China (61975100, 62027821, 62105192); Research Project Supported by Shanxi Scholarship Council of China (2022-015); Fund for Shanxi "1331 Project" Key Subjects Construction; Program for the Innovative Talents of High Education Institutions of Shanxi; First Lab-National Innovation Center (Shanxi) Science and Technology Innovation Project; Shanxi Province Patent Conversion Project (202305007); Special Fund for Science and Technology Innovation Teams of Shanxi Province (202204051002005); Applied Basic Research Project of Shanxi Province (202103021221004).

Disclosures. The authors declare no conflicts of interest.

Data availability. Data underlying the results presented in this paper are not publicly available at this time but may be obtained from the authors upon reasonable request.

REFERENCES

1. Y. Huang, B. Liu, L. Peng, *et al.*, Nat. Commun. **2**, 546 (2011).
2. L. Winkelmann, *Injection-Locked High Power Oscillator for Advanced Gravitational Wave Observatories* (Cuvillier Verlag Göttingen, 2012).
3. C. Robin, I. Dajani, and B. Pulford, Opt. Lett. **39**, 666 (2014).
4. X. Zhang, J. Ye, X. Luo, *et al.*, Opt. Express **29**, 5687 (2021).
5. F. Saltarelli, A. Diebold, I. J. Graumann, *et al.*, Optica **5**, 1603 (2018).
6. N. Bode, F. Meylahn, and B. Willke, Opt. Express **28**, 29469 (2020).
7. X. Délen, S. Piehler, J. Didierjean, *et al.*, Opt. Lett. **37**, 2898 (2012).
8. S. Chen, Q. Na, C. Xu, *et al.*, Opt. Lett. **47**, 674 (2022).
9. Q. He, Z. Zhao, X. Ye, *et al.*, Micromachines **13**, 324 (2022).
10. W. A. Clarkson, J. Phys. D: Appl. Phys. **34**, 2381 (2001).
11. N. Hodgson and H. Weber, IEEE J. Quantum Electron. **29**, 2497 (1993).
12. S. Chénais, F. Druon, S. Forget, *et al.*, Prog. Quantum Electron. **30**, 89 (2006).
13. A. M. Bonnefois, M. Gilbert, P.-Y. Thro, *et al.*, Opt. Commun. **259**, 223 (2006).
14. A. M. Rodin, A. Aleknavicius, A. Michailovas, *et al.*, Proc. SPIE **9342**, 934207 (2015).
15. Y. Wei, W. Peng, J. Li, *et al.*, Opt. Lett. **48**, 676 (2023).